

# Tradeoffs between Gate Oxide Leakage and Delay for Dual $T_{ox}$ Circuits\*

Anup Kumar Sultania  
Department of ECE  
University of Minnesota  
Minneapolis, MN 55455.  
anups@ece.umn.edu

Dennis Sylvester  
Department of EECS  
University of Michigan  
Ann Arbor, MI 48109.  
dennis@eecs.umich.edu

Sachin S. Sapatnekar  
Department of ECE  
University of Minnesota  
Minneapolis, MN 55455.  
sachin@ece.umn.edu

## ABSTRACT

Gate oxide tunneling current ( $I_{gate}$ ) will become the dominant component of leakage in CMOS circuits as the physical oxide thickness ( $T_{ox}$ ) goes below 15Å. Increasing the value of  $T_{ox}$  reduces the leakage at the expense of an increase in delay, and a practical tradeoff between delay and leakage can be achieved by assigning one of the two permissible  $T_{ox}$  values to each transistor. In this paper, we propose an algorithm for dual  $T_{ox}$  assignment to optimize the total leakage power under delay constraints, and generate a leakage/delay trade-off curve. As compared to the case where all transistors are set to low  $T_{ox}$ , our approach achieves an average leakage reduction of 83% under 100nm models.

## Categories and Subject Descriptors

B.7.2 [Hardware]: Integrated Circuits—*design aids*

## General Terms

Performance, Algorithms

## Keywords

Leakage power, Dual  $T_{ox}$  Circuits

## 1. INTRODUCTION

Leakage current is a primary concern for low power, high performance digital CMOS circuits for portable applications, and industry trends show that leakage will be the dominant component of power in future technologies. New leakage mechanisms, such as tunneling across thin gate oxides, which lead to gate oxide leakage current ( $I_{gate}$ ), are coming into play from the 90nm node onwards.

According to the International Technological Roadmap for Semiconductors (ITRS) [1], physical oxide thickness ( $T_{ox}$ ) values of 7–12Å will be required for high performance CMOS circuits by 2006, and quantum effects that cause tunneling will play a dominant role in such ultra-thin oxide devices. The probability of electron tunneling is a strong function

of the barrier height (i.e., the voltage drop across gate oxide) and the barrier thickness, which is simply  $T_{ox}$ , and a small change in  $T_{ox}$  can have a tremendous impact on  $I_{gate}$ . For example, in MOS devices with SiO<sub>2</sub> gate oxides, a difference in  $T_{ox}$  of only 2Å can result in an order of magnitude increase in  $I_{gate}$  [2], so that reducing  $T_{ox}$  from 18Å to 12Å increases  $I_{gate}$  by approximately 1000×. The other component of leakage, subthreshold leakage ( $I_{sub}$ ), forms a reducing fraction of the total leakage as  $T_{ox}$  is reduced, so that  $I_{gate}$  will become the dominant leakage mechanism in the future. The most effective way to control  $I_{gate}$  would be through the use of high- $k$  dielectrics, but such materials are not expected before the 65nm technology node in 2007, at the earliest.

This paper will explore the use of dual  $T_{ox}$  values for performance optimization. Although this optimization can be exploited at a number of points in the design methodology, our solution considers  $T_{ox}$  assignment as a step that is performed after placement and transistor sizing, at which point it is used to achieve a final performance improvement. Unlike earlier stages of design, there is less design uncertainty at this point and minor changes in layout parasitics due to  $T_{ox}$  assignment can be dealt with an incremental update. As a result, all of the delay gains from our procedure can be guaranteed in the final design, with a low leakage power overhead.

Leakage power can be broadly divided into two categories: *standby leakage*, which corresponds to the situation when the circuit is in a non-operating or sleep mode, and *active leakage*, which relates to leakage during normal operation. Numerous effective techniques for controlling standby leakage have been proposed in the past, including state assignment [3], the use of multiple threshold CMOS (MTCMOS) sleep transistors [4], body-biasing [5], and dual  $T_{ox}$  combined with state assignment. Active leakage, however, has not been addressed very widely in the literature so far, primarily because it has not been a major issue in the present technologies. However, leakage power dissipation in the active mode has grown to over 40% in some high-end parts today [6]. Therefore, reducing active leakage is vital for advanced technologies in current-generation circuits, and for next-generation technologies. The range of options that are available for reducing active leakage is considerably more limited than for standby leakage, and the use of dual  $T_{ox}$  assignments is a powerful method for this purpose.

Prior research related to our work is summarized as follows. In [7], the authors examine the interaction between  $I_{gate}$  and  $I_{sub}$ , and their state dependencies. This work ap-

\*This work was supported in part by the SRC under contract 2003-TJ-1092, and by the NSF under award CCR-0205227.

Permission to make digital or hard copies of all or part of this work for personal or classroom use is granted without fee provided that copies are not made or distributed for profit or commercial advantage and that copies bear this notice and the full citation on the first page. To copy otherwise, to republish, to post on servers or to redistribute to lists, requires prior specific permission and/or a fee.

DAC 2004, June 7–11, 2004, San Diego, California, USA.  
Copyright 2004 ACM 1-58113-828-8/04/0006 ...\$5.00.

plies pin reordering to minimize  $I_{gate}$ . The impact of  $I_{gate}$  on delay is discussed in [8], but its impact on leakage power is not addressed. The work in [9] presents an approach to reducing  $I_{sub}$ , but not  $I_{gate}$ , using separate optimizations to select the values of  $T_{ox}$ .

In our context, where we optimize the total leakage, comprising both  $I_{gate}$  and  $I_{sub}$ , the rationale for optimizing  $T_{ox}$  is as follows. Choosing a lower value of  $T_{ox}$  can result in lower delays, but at the cost of increased leakage, and the value of  $T_{ox}$  can therefore be optimized to obtain a leakage/delay tradeoff. For practical reasons, it is important to scale the effective channel length  $L_{eff}$  along with  $T_{ox}$  [10].

Due to process constraints, rather than an unlimited range of  $T_{ox}$  values, it is more reasonable to choose between two permissible values. In Section 2, we describe a method for selecting appropriate values of the low and high values of the oxide thickness, referred to as  $T_{oxLo}$  and  $T_{oxHi}$ , respectively, and the corresponding values for the channel length. Next, in Sections 3 and 4, respectively, we introduce the leakage and delay models that are used in this work, and demonstrate that they show a good degree of accuracy as compared to simulation results. Our iterative algorithm for finding the leakage/delay tradeoff is then presented in Section 5, followed by a description of our experimental results in Section 6 and concluding remarks in Section 7.

## 2. CHOOSING $T_{ox}$ AND $L_{eff}$

While an increased value of  $T_{ox}$  succeeds in significantly reducing  $I_{gate}$ , several other physical effects must be taken into consideration. Increasing the value of  $T_{ox}$  while keeping the channel length constant may adversely impact the functionality of the transistor. Specifically, due to drain induced barrier lowering (DIBL), an increase in  $T_{ox}$  may result in a situation where the drain terminal takes control of the channel, so that the “on” or “off” state of the transistor is no longer completely governed by the gate terminal.

This effect has been recognized during technology scaling, and scaling trends have shown that  $T_{ox}$  reduces nearly in proportion with  $L_{eff}$  [11]. We maintain this proportion for each of the chosen values of  $T_{ox}$  by setting

$$\frac{L_{eff}@T_{oxLo}}{T_{ox,eLo}} = \frac{L_{eff}@T_{oxHi}}{T_{ox,eHi}} \quad (1)$$

The term  $T_{ox,e}$  in this equation refers to the *electrical*  $T_{ox}$ , which is related to the *physical* value of  $T_{ox}$  as follows<sup>1</sup>

$$T_{ox,e} = T_{ox} + T_{oxoffset} \quad (2)$$

The  $T_{oxoffset}$  term is added to account for the gate depletion and channel quantization effects, and a typical value is 0.7nm [12]. In the remainder of this paper, it will be implicit that as we change  $T_{ox}$ , the value of  $L_{eff}$  will also be scaled.

Before determining reasonable values for  $T_{oxLo}$  and  $T_{oxHi}$ , we will study the effect of varying  $T_{ox}$  on leakage for an inverter. The gate oxide leakage,  $I_{gate}$ , and the subthreshold leakage,  $I_{sub}$ , for both the NMOS and PMOS transistors in the inverter, are graphically depicted in Figure 1(a) for various values of  $T_{oxHi}$ , at  $T_{oxLo} = 12\text{\AA}$ ; the sum of these components is shown by the bottommost curve in Figure 1(b). The values of  $I_{sub}$  are obtained through SPICE simulations on predictive technology models [13], and an analytical model (described in Section 3.2) is used to generate

<sup>1</sup>Henceforth, our discussions will be with reference to  $T_{ox}$ , the *physical* value of the gate oxide thickness.

$I_{gate}$ <sup>2</sup>. The average leakage of the inverter is calculated as the sum of the average  $I_{gate}$  and  $I_{sub}$  leakages (as described in greater detail in Section 3), and is shown in Figure 1(b).

As  $T_{ox}$  is varied,  $I_{sub}$  shows a negligible change in comparison to  $I_{gate}$ . Furthermore, the average leakage decreases slowly for  $T_{ox} > 17\text{\AA}$ , and increases sharply as  $T_{ox}$  goes below  $17\text{\AA}$ . On the other hand, the delay of the inverter (as will be seen by the experiment in Figure 2) increases linearly with  $T_{ox}$ , so that using a value of  $T_{oxHi}$  of over  $17\text{\AA}$  results in a larger delay with no appreciable savings in the leakage. This leads us to choose  $T_{oxHi} = 17\text{\AA}$ .

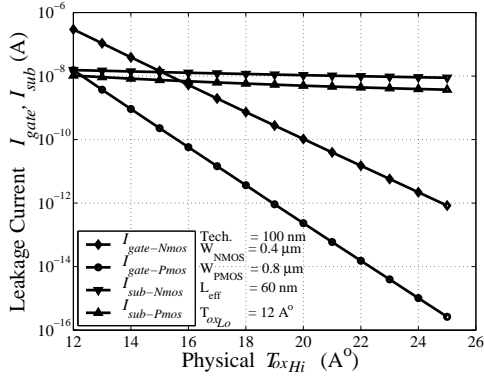
To choose  $T_{oxLo}$ , we consider several scenarios as shown by the plots in Figure 1(b). Each curve corresponds to a different choice of  $T_{oxLo}$ , and the value of  $L_{eff}$  is set to 60nm at this value. Each point on a curve now shows the total leakage for an inverter whose transistors are set to a candidate value of  $T_{oxHi}$ . For instance, for the curve where  $T_{oxLo} = 15\text{\AA}$ , candidate values for  $T_{oxHi}$  range from  $28\text{\AA}$  to  $15\text{\AA}$ , and the  $L_{eff}$  value for each case is scaled in accordance with Equation (1). It is easily seen that on each curve, the  $T_{ox}$  value at which the leakage begins to change at exponential rate is about  $17\text{\AA}$ . In other words, for the entire range of  $T_{oxLo}$  candidate values of  $12\text{\AA}$  through  $15\text{\AA}$ , it is clear that our choice of  $T_{oxHi} = 17\text{\AA}$  is reasonable. For a wider range of delay values in the tradeoff curve, the difference in  $T_{oxLo}$  and  $T_{oxHi}$  should be as high as possible. The choice of  $T_{oxLo}$ , however, is limited by  $I_{gate}/I_{sub}$  ratio. This ratio, at  $T_{oxLo}$ , should be such that  $I_{gate}$  does not completely dwarf  $I_{sub}$ . Furthermore, due to process variation in  $T_{ox}$ , the choice of  $T_{oxLo}$  and  $T_{oxHi}$  should be such that their probability distribution functions do not overlap. We choose  $T_{oxLo} = 12\text{\AA}$  as it gives the best achievable leakage/delay tradeoff.

We now consider the impact of changing  $T_{ox}$  and  $L_{eff}$  on the gate capacitance,  $C_{inv}$ , and the threshold voltage,  $V_{th}$ , of the MOS devices; each of these parameters clearly depends on  $T_{ox}$  and  $L_{eff}$ . We perform a set of SPICE simulations on a circuit set-up illustrated in Figure 2. In this experiment, the  $T_{ox}$  value of Inverter 2 is varied, and all other inverters are maintained at a fixed  $T_{ox}$  value of  $17\text{\AA}$ . The results are shown in the table in the same figure, and lead to a happy coincidence. Our method of scaling the value of  $L_{eff}$  linearly with  $T_{ox}$  results in a *nearly constant* values of  $C_{inv}$  and  $V_{th}$ , respectively. However, there is a noticeable impact on the gate delay: increasing  $T_{ox}$  and  $L_{eff}$  decreases the channel transconductance, and hence increases the delays. Changing  $T_{ox}$  from  $12\text{\AA}$  to  $22\text{\AA}$  alters the delays *linearly*, with a delay penalty of 51% over this range for Inverter 2.

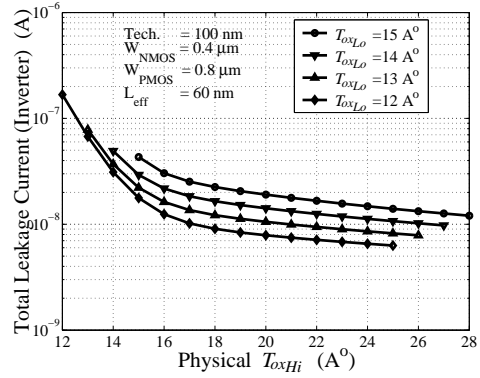
The invariance of the capacitance of Inverter 2 over the entire range of  $T_{ox}$  has two notable consequences:

- A change in  $T_{ox}$  of a transistor leaves the load capacitance presented to the previous stage of logic unchanged. As a result, the delay of a fanin logic gate does not change significantly, and hence our optimization method needs only to consider the delay change of a given logic gate when its  $T_{ox}$  is altered.
- Since the capacitance is unchanged, the  $CV_{dd}^2f$  (dynamic) power remains unaffected by changes in  $T_{ox}$ . This is extremely important since our optimization targets the active mode of operation.

<sup>2</sup>We cannot use simulations here since the Berkeley predictive technology model [13] uses BSIM3, which does not model  $I_{gate}$ .

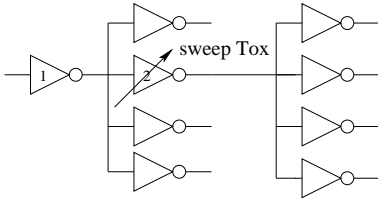


(a)



(b)

**Figure 1:** (a) The four leakage components for an inverter ( $I_{gate}$  and  $I_{sub}$  for the NMOS and PMOS transistors, respectively) as a function of the gate oxide thickness. (b) The total leakage of an inverter for different values of  $T_{oxLo}$  and  $T_{oxHi}$ . At each point,  $L_{eff}$  is scaled with respect to the minimum  $T_{ox}$  value on the curve; at this point,  $L_{eff} = 60\text{nm}$ .



| $T_{ox}$ (Å) | $L_{eff}$ (nm) | $D_{Inv1}$ (ps) | $D_{Inv2}$ (ps) | $C_{inv}$ (fF) | $V_{th}$ (V) |
|--------------|----------------|-----------------|-----------------|----------------|--------------|
| 12           | 60.0           | 33.84           | 33.56           | 1.98           | 0.119        |
| 14           | 66.3           | 33.77           | 36.70           | 1.99           | 0.120        |
| 16           | 72.6           | 33.71           | 39.98           | 1.99           | 0.122        |
| 18           | 78.9           | 33.67           | 43.40           | 1.99           | 0.124        |
| 20           | 85.2           | 33.64           | 46.97           | 2.00           | 0.126        |
| 22           | 91.6           | 33.62           | 50.69           | 2.00           | 0.127        |

**Figure 2:** The effect of varying  $T_{ox}$  of Inverter 2 on (i) its delay and on delay of its fanin gate, Inverter1 (ii) the input capacitance of the inverter  $C_{inv}$  (calculated as the sum of the NMOS and PMOS gate capacitances), and (iii) the threshold voltage  $V_{th}$  of the NMOS device. The transistor widths are chosen as  $W_n = 0.4\mu\text{m}$  and  $W_p = 0.8\mu\text{m}$ .

### 3. LEAKAGE MODELS

We will now describe the models used to calculate  $I_{sub}$  and  $I_{gate}$  for each transistor, and the approach for computing the average  $I_{sub}$  and  $I_{gate}$  values for a given logic gate. The total leakage current for a logic gate is then computed as the sum of its corresponding average  $I_{sub}$  and  $I_{gate}$ .

#### 3.1 Subthreshold Leakage Model

As seen in the table in Figure 2, the value of  $V_{th}$  changes by a very small amount as  $T_{ox}$  is changed. In spite of this, it can have significant effects on  $I_{sub}$ , which is exponentially dependent on  $V_{th}$ . For convenience, we use a simple look-up table (LUT) to determine  $I_{sub}$ . Conceptually, such an LUT could be extremely large: for a  $k$ -input NAND gate, for instance, we would store the leakage current for each of the  $2^k$  possible  $T_{ox}$  assignments<sup>3</sup>, and each  $T_{ox}$  assignment would require entries for the  $2^k - 1$  leakage states corresponding to different input logic values<sup>4</sup>, resulting in a total of  $2^k \cdot (2^k - 1)$  entries. The LUT size can be reduced significantly using the following ideas:

**Dominant input states:** It has been shown [14] that  $I_{sub}$  can be accurately captured by using a set of dominant states, corresponding to the cases where only one transistor on each path to a supply node is on.

**Weak  $T_{ox}$  dependencies:** In a dominant state, for a given  $T_{ox}$  choice for the leaking transistor the subthreshold

leakage is only weakly dependent on the  $T_{ox}$  values of other transistors. Intuitively, this relates to the fact that the leaking transistor is the largest resistance on the path. We have validated this through SPICE simulations, and the results for a 4-input NAND gate are shown in Figure 3. When  $T_4$  is the leaking transistor and is set to  $T_{oxLo}$ , it can be seen that  $I_{sub}$  has a range of only about 1% over all possible assignments for the other inputs. Similar results are seen for other logic gates over various  $T_{ox}$  assignments.

For a  $k$ -input NAND gate, there are  $k$  dominant states. The weak  $T_{ox}$  dependencies require that for each of these states, two  $I_{sub}$  numbers must be maintained: one at  $T_{oxHi}$  and one at  $T_{oxLo}$ . As a result, the LUT size comes down to  $2k$ .

For a logic gate with  $k$ -parallel transistors (such as the pull-up in a  $k$ -input NAND, or a pull-down in a  $k$ -input NOR), 2 entries ( $T_{oxHi}$  and  $T_{oxLo}$ ) are sufficient as the value of  $I_{sub}$  per unit  $\frac{W}{L}$  for each parallel branch is almost equal.

The average subthreshold leakage ( $I_{sub,avg}$ ) for a logic gate under a given  $T_{ox}$  assignment may therefore be calculated as follows:

$$I_{sub,avg} = \sum_{i \in \text{dominant input states}} P_i \times I_{sub_i} \quad (3)$$

where  $P_i$  is the probability of occurrence of state  $i$ , and  $I_{sub_i}$  is the subthreshold leakage current in that state.

#### 3.2 Gate Oxide Tunneling Model

Gate oxide leakage can be primarily attributed to electron [hole] tunneling in NMOS [PMOS] devices. Physically, this tunneling occurs in the gate-to-channel region, and in the gate-to-drain/source overlap regions. The latter type

<sup>3</sup>Series-connected devices can have different  $T_{ox}$  provided they are spaced out a little more than the design rules indicate.

<sup>4</sup>The only input assignment with no leakage due to NMOS is the case when all transistors in the pull-down chain are on.

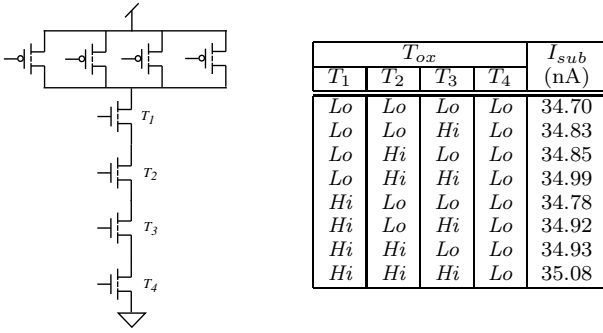


**Figure 3:** The variation of  $I_{sub}$  through the pull-down chain for the dominant state when only  $T_4$  is off. Here,  $T_{oxLo} = 12\text{\AA}(Lo)$ ,  $T_{oxHi} = 17\text{\AA}(Hi)$ , and  $T_4$  is at  $T_{oxLo}$ .

of tunneling, referred to as edge direct tunneling (EDT) is ignored in our case for two reasons: firstly, because the gate-to-drain/source overlap region is significantly smaller than the channel region, and secondly, because the oxide thickness in this overlap region can be increased after gate patterning to further suppress EDT [15].

Our work focuses on gate-to-channel tunneling, and we use the following analytic tunneling current density ( $J_{tunnel}$ ) model based on the electron [hole] tunneling probability through a barrier height ( $E_B$ ) [16].

$$J_{tunnel} = \frac{4\pi m^* q}{h^3} (kT)^2 \left(1 + \frac{\gamma kT}{2\sqrt{E_B}}\right) \times \exp\left(\frac{E_{F0,Si/SiO_2}}{kT}\right) \exp(-\gamma\sqrt{E_B}) \quad (4)$$

where  $E_{F0,Si/SiO_2}$  is the Fermi level at the Si/SiO<sub>2</sub> interface and  $m^*$  is  $0.19M_o$  for electron tunneling and  $0.55M_o$  for hole tunneling, where  $M_o$  is the electron rest mass. The terms  $k$ ,  $h$  and  $q$  correspond to physical constants (respectively, Boltzmann's constant, Planck's constant and the charge on an electron),  $\gamma = 4\pi T_{ox}\sqrt{2M_{ox}}/h$  where  $M_{ox}$  is the effective electron [hole] mass in the oxide,  $T$  is the operating temperature, and  $E_B$  is the barrier height.

It was shown in [7] that like  $I_{sub}$ ,  $I_{gate}$  also exhibits state dependency. When the gate node of the transistor is at logic 0, the only possible tunneling component is EDT, which is neglected in our work; therefore, we will only consider the cases where the gate node is at logic 1. For example, while determining  $I_{gate}$  for transistor  $T_2$  in the 4-input NAND gate in Figure 3, it can be shown that the maximum leakage for  $T_2$  occurs at the input state<sup>5</sup>  $(x, 1, 1, 1)$ , and that the  $I_{gate}$  values for the states  $(1, 1, 0, x)$ ,  $(0, 1, 0, x)$  and  $(x, 1, 1, 0)$  can be ignored. For details, the reader is referred to [7].

In general, this may be restated as follows: the dominant state for  $I_{gate}$  for a particular transistor in a stack corresponds to the case when all of the transistors below (above) it in the NMOS (PMOS) stack are on. The average  $I_{gate}$  for a logic gate can then be calculated as:

$$I_{gate,avg.} = \sum_{\text{transistor } i \in \text{logic gate}} P_i \times I_{gate_i} \quad (5)$$

Here,  $P_i$  for NMOS [PMOS] transistors connected in parallel, as in a NOR [NAND] gate, is the probability that the input is at logic 1 [0]. For a stack of NMOS [PMOS] transistors in series in a NAND [NOR] gate,  $P_i$  for a transistor is the product of the probabilities that each of the transistors below [above] it have an input of logic 1 [0]. The value of

<sup>5</sup>“State” = logic values at the inputs to  $(T_1, T_2, T_3, T_4)$ .

|       | $T_{ox}$ |       |       |       | Delay |       |         |
|-------|----------|-------|-------|-------|-------|-------|---------|
|       | $T_1$    | $T_2$ | $T_3$ | $T_4$ | Spice | LUT   | Error   |
| $D_0$ | Lo       | Lo    | Lo    | Lo    | 13.89 | —     | —       |
| $D_1$ | Lo       | Lo    | Lo    | Hi    | 14.84 | 14.51 | -2.22 % |
| $D_2$ | Lo       | Lo    | Hi    | Lo    | 14.21 | 14.51 | 2.11 %  |
| $D_3$ | Hi       | Lo    | Lo    | Lo    | 14.54 | 14.51 | -0.21 % |
| $D_4$ | Lo       | Lo    | Hi    | Hi    | 15.11 | 15.13 | 0.13 %  |
| $D_5$ | Hi       | Lo    | Lo    | Hi    | 15.47 | 15.13 | -2.20 % |
| $D_6$ | Hi       | Lo    | Hi    | Lo    | 14.86 | 15.13 | 1.82 %  |
| $D_7$ | Hi       | Lo    | Hi    | Hi    | 15.75 | —     | —       |

**Table 1:** Delays from the input of switching transistor  $T_2$  in a 4-input NAND [Figure 3] @ $T_{oxLo} = 12\text{\AA}$ ,  $T_{oxHi} = 17\text{\AA}$ .

$I_{gate}$  is computed using Equation (4) for the specified  $L_{eff}$  and width of the transistor under consideration.

Observe that the use of dominant states for the computation of  $I_{gate}$  and  $I_{sub}$  automatically rules out the complex interaction between these two components, as in [7].

## 4. DELAY MODEL

For advanced nanometer technologies, it is difficult to obtain accurate closed-form delay models, and therefore, we use an LUT-based approach for the delay. For each input of the logic gate, rise and fall delay values are determined through SPICE simulations over a range of output loads under a single-input switching model. A linear fit is carried out on these data to obtain the slope (delay/load) and intercept (delay at zero load) values. The LUT stores these two numbers for each input, along with gate input capacitance for each logic gate. The output load for a logic gate can be computed by summing up the input gate capacitance of the fanout logic gates. Based on this load, the delay of the logic gate is calculated as:

$$Delay = Intercept + Slope \times Load \quad (6)$$

Different combinations of  $T_{ox}$  in a stack of transistors will result in different input-to-output delays for the same input; for example, for a  $k$ -input NAND gate,  $2^k$  entries would be required to compute the fall delay from each input to the output, for a total of  $k \cdot 2^k$  entries in the LUT. This LUT size may be greatly reduced for a small loss in accuracy.

For the output fall transition, for each input-to-output delay, we create two LUT's, corresponding to a gate oxide thickness assignment of  $T_{oxLo}$  and  $T_{oxHi}$ , respectively; similarly, two LUT's are constructed for the rise transition. In each LUT, we observe that the delay depends strongly on the number of transistors in the chain that are at  $T_{oxLo}$  or  $T_{oxHi}$ , and very weakly on their position. This is illustrated for a 4-input NAND gate in Table 1 for the delay from the input of  $T_4$  to the output. We fit a simple formula as follows:

$$Delay = D_0 + n \times \frac{(D_7 - D_0)}{3} \quad (7)$$

where  $D_0$  and  $D_7$  are delay values (stored in the LUT) for the extreme cases of non-switching transistors being at all  $T_{oxLo}$  and all  $T_{oxHi}$ , respectively, as shown in Table 1, and  $n$  is the number of transistors (other than the switching transistor) at  $T_{oxHi}$ . The errors under this method are shown in Table 1. Therefore, all possible fall delay scenarios for a  $k$ -input NAND gate can be compacted into  $4k$  LUT entries. This technique was applied to several gate types, and in most cases, the error was under 2%, with a worst-case error of 3%.

A similar compression for the case of output rise LUT's of a  $k$ -input NAND is possible. Since the PMOS transistors are in parallel, only the gate-to-drain overlap capacitance at the output node changes for different  $T_{ox}$  combinations for the transistors; this has an insignificant impact on the delay, and hence,  $2k$  LUT entries (corresponding to  $T_{ox_{Hi}}$  and  $T_{ox_{Lo}}$  for each PMOS input) are sufficient.

A similar approach can be applied to build LUT's for a  $k$ -input NOR gate, and for other types of logic gates. Therefore, the total number of LUT entries varies linearly with the number of inputs to the logic gate. The input transition time can be accounted for in this model by creating one such LUT for each candidate transition time.

## 5. DUAL $T_{ox}$ ASSIGNMENT

We use a TILOS-like [17] sensitivity-based heuristic for assigning  $T_{ox}$  values to individual transistors in a circuit. Starting with all transistors at  $T_{ox_{Hi}}$ , the heuristic (Algorithm 1) performs a static timing analysis step. Next, it greedily identifies the transistor on the critical path that, when changed to  $T_{ox_{Lo}}$ , would cause the largest delay reduction for the smallest increase in leakage. These two steps iterate until no further improvement is possible, and a leakage-delay tradeoff curve is thus obtained.

A standard static timing analysis (STA) approach is used to find the critical path. The propagation delay  $D_p$  for each gate is computed using the LUT described in Section 4. In principle, the STA must be repeated after each  $T_{ox}$  change; however, we observe that every such  $T_{ox}$  change is local and only changes delays and arrival times in its transitive fanout region. Therefore, after the first iteration, we achieve efficiency by performing incremental STA that processes only the affected regions.

```

{Circuit is represented as an acyclic graph  $G(V, E)$ }
{The target delay is  $D_T$ }
Initialize all transistors to  $T_{ox_{Hi}}$ 
Propagate state probabilities from PI's to internal nodes
for each node  $x \in G(V, E)$  do
  Find output load =  $\sum$  fanout nodes gate capacitance
  Get rise, fall delays ( $D_{P_{fall}}, D_{P_{rise}}$ ) from delay LUT
  Find  $I_{sub}, I_{gate}$  based on LUT's
end for
Perform STA to find rise and fall  $AT, RT$  for each node
and circuit delay,  $D_{max}$ 

while  $D_{max} > D_T$  do
   $(\frac{\Delta D}{\Delta Lkg})_{worst} = 0; N_{chosen} = \text{NULL};$ 
  for each node  $y$  on a critical path do
    if (critical path transistor(s) of  $y == T_{ox_{Hi}}$ ) then
      find  $(\frac{\Delta D}{\Delta Lkg})_y$  for node  $y$ 
      if  $(\frac{\Delta D}{\Delta Lkg})_{worst} > (\frac{\Delta D}{\Delta Lkg})_y$  then
         $(\frac{\Delta D}{\Delta Lkg})_{worst} = (\frac{\Delta D}{\Delta Lkg})_y; N_{chosen} = y$ 
        {Tie-breakers: #fanouts, proximity to PI}
      end if
    end if
  end for
  if  $(\frac{\Delta D}{\Delta Lkg})_{worst} \neq 0$  then
    Assign  $T_{ox_{Lo}}$  to the worst transistor in  $N_{chosen}$ 
    Update  $D_{P_{fall}}, D_{P_{rise}}, I_{sub}, I_{gate}$  of  $N_{chosen}$ 
    Perform Incremental STA and recalculate  $D_{max}$ 
  else
    Report  $D_{max}; \text{Exit}()$ 
  end if
end while

```

**Algorithm 1:** Pseudocode for Dual  $T_{ox}$  Assignment

Once this critical path is found, the core of the optimizer iteratively changes one transistor on this path from  $T_{ox_{Hi}}$  to  $T_{ox_{Lo}}$  in each iteration. This transistor is identified by measuring the increase in the total average leakage,  $\Delta Lkg$ , with respect to the delay reduction,  $\Delta D$ , of the critical path when such a change is made. In other words, we evaluate

$$Cost = \frac{\Delta D}{\Delta Lkg} \quad (8)$$

The transistor with the minimum (most negative) cost provides the largest delay reduction for the smallest increase in leakage power, and is selected for assignment to  $T_{ox_{Lo}}$ . The corresponding  $L_{eff}$  is also concurrently changed. If two transistors have the same cost, ties are heuristically broken, first by selecting the transistor with the higher fanout, and if that fails, then by choosing the one that is closer to the PI (since it has a larger cone of influence, and is likely to reduce the delay on a larger number of paths).

In evaluating  $\Delta D$ , it is enough to find the delay change of the logic gate that the transistor belongs to. Since changes in  $T_{ox}$  leave the transistor input capacitance unchanged (see Section 2), the delay of the fanin gate is unchanged.

## 6. EXPERIMENTAL RESULTS

The proposed method for optimizing the total leakage was applied to the ISCAS85 benchmarks, and leakage/delay tradeoff curves were generated. A library consisting of inverter, and Nand and Nor gates with 2, 3, and 4 inputs, was characterized for a 100nm technology node using SPICE simulations based on a predictive model [13]. Based on this library, circuits were synthesized using SIS [18]. We used  $V_{dd} = 1.2V$ , inverter transistor widths  $W_n = 400nm/W_p = 800nm$  (the widths for other gates are accordingly scaled),  $T_{ox_{Lo}} = 12\text{\AA}$ , and  $T_{ox_{Hi}} = 17\text{\AA}$  in our experimental setup.

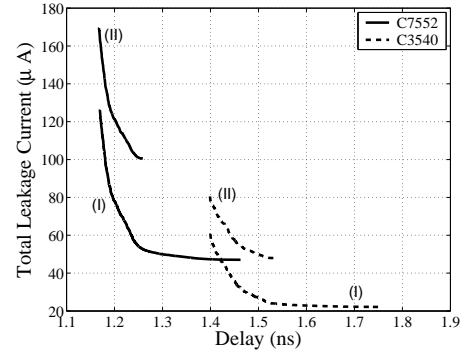


**Figure 4:** Leakage/Delay tradeoff curve for C2670 and C3540 with (I) all transistor  $T_{ox}$ 's optimized (II) all PMOS devices fixed at  $T_{ox_{Lo}}$  and all NMOS  $T_{ox}$ 's optimized.

Tradeoff curves for two representative benchmarks are shown in Figure 4. All of the curves (only two are shown due to space constraints) show a knee region that corresponds to a good design point. The points to the right of the knee incur a large delay penalty for a little reduction in total leakage, while those on the left have a large leakage overhead for minor delay benefits. A notable observation is that though  $I_{gate}$  of a single PMOS transistor is small, setting all PMOS transistors to  $T_{ox_{Lo}}$  incurs a high cumulative expense. This is shown by the curves (II), which correspond to a case where all PMOS transistors are set to  $T_{ox_{Lo}}$  and the  $T_{ox}$  values of only the NMOS devices are optimized. This curve is clearly inferior to the curves (I) that correspond to a full  $T_{ox}$  optimization for all NMOS and PMOS transistors.

| Circuit | Delay |        | Leakage Current ( $\mu A$ ) |            |                  | CPU Time (s) | Circuit | Delay |        | Leakage Current ( $\mu A$ ) |            |                  | CPU Time (s) |
|---------|-------|--------|-----------------------------|------------|------------------|--------------|---------|-------|--------|-----------------------------|------------|------------------|--------------|
|         | (ns)  | (%D)   | $I_{sub}$                   | $I_{gate}$ | $I_{total}$ (%R) |              |         | (ns)  | (%D)   | $I_{sub}$                   | $I_{gate}$ | $I_{total}$ (%R) |              |
| C432    | 1.26  | (24.6) | 3.77                        | 0.69       | 4.46             | 2.2          | C499    | 0.93  | (25.4) | 7.28                        | 1.61       | 8.89             | 11           |
|         | 1.14  |        | 3.90                        | 1.02       | 4.92             |              |         | 0.84  |        | 7.57                        | 2.48       | 10.05            |              |
|         | 1.09  |        | 4.02                        | 2.08       | 6.10             |              |         | 0.80  |        | 7.84                        | 4.54       | 12.38            |              |
|         | 1.04  |        | 4.14                        | 4.83       | 8.97             |              |         | 0.77  |        | 8.10                        | 27.45      | 35.55            |              |
|         | 1.01  |        | 4.22                        | 14.01      | 18.24 (83.8)     |              |         | 0.74  |        | 8.34                        | 67.98      | 76.32 (70.2)     |              |
|         | 1.01  |        | 5.17                        | 107.53     | 112.70           |              |         | 0.74  |        | 9.92                        | 246.20     | 256.12           |              |
| C880    | 0.85  | (25.5) | 5.00                        | 1.16       | 6.16             | 1.4          | C1355   | 1.03  | (25.0) | 7.42                        | 1.68       | 9.09             | 12           |
|         | 0.75  |        | 5.07                        | 1.34       | 6.41             |              |         | 0.93  |        | 7.72                        | 2.96       | 10.67            |              |
|         | 0.72  |        | 5.12                        | 1.93       | 7.06             |              |         | 0.88  |        | 7.93                        | 5.87       | 13.81            |              |
|         | 0.69  |        | 5.17                        | 4.12       | 9.29             |              |         | 0.84  |        | 8.16                        | 36.13      | 44.28            |              |
|         | 0.68  |        | 5.21                        | 9.11       | 14.31 (92.3)     |              |         | 0.82  |        | 8.38                        | 77.06      | 85.43 (67.9)     |              |
|         | 0.68  |        | 6.83                        | 179.14     | 185.97           |              |         | 0.82  |        | 9.93                        | 256.36     | 266.30           |              |
| C1908   | 1.34  | (25.2) | 8.89                        | 2.09       | 10.99            | 12           | C2670   | 1.20  | (25.3) | 12.37                       | 3.32       | 15.69            | 9.4          |
|         | 1.21  |        | 9.16                        | 2.98       | 12.14            |              |         | 1.06  |        | 12.53                       | 4.00       | 16.53            |              |
|         | 1.15  |        | 9.42                        | 6.71       | 16.13            |              |         | 1.02  |        | 12.70                       | 5.86       | 18.56            |              |
|         | 1.11  |        | 9.63                        | 20.27      | 29.89            |              |         | 0.99  |        | 12.86                       | 10.07      | 22.93            |              |
|         | 1.07  |        | 9.78                        | 49.10      | 58.88 (82.3)     |              |         | 0.96  |        | 12.97                       | 25.74      | 38.72 (92.6)     |              |
|         | 1.07  |        | 12.19                       | 321.42     | 333.61           |              |         | 0.95  |        | 16.90                       | 506.69     | 523.59           |              |
| C3540   | 1.75  | (25.1) | 17.63                       | 4.51       | 22.13            | 22           | C5315   | 1.59  | (26.1) | 27.71                       | 7.37       | 35.08            | 36           |
|         | 1.56  |        | 17.94                       | 5.43       | 23.37            |              |         | 1.43  |        | 28.07                       | 8.22       | 36.29            |              |
|         | 1.49  |        | 18.20                       | 9.36       | 27.55            |              |         | 1.36  |        | 28.35                       | 11.30      | 39.66            |              |
|         | 1.44  |        | 18.43                       | 21.22      | 39.64            |              |         | 1.31  |        | 28.63                       | 26.33      | 54.96            |              |
|         | 1.40  |        | 18.64                       | 42.67      | 61.31 (91.4)     |              |         | 1.26  |        | 28.82                       | 68.59      | 97.41 (91.7)     |              |
|         | 1.40  |        | 23.99                       | 691.55     | 715.54           |              |         | 1.26  |        | 37.84                       | 1128.85    | 1166.7           |              |
| C6288   | 4.75  | (25.7) | 36.88                       | 8.95       | 45.82            | 258          | C7552   | 1.46  | (25.3) | 37.60                       | 9.46       | 47.06            | 127          |
|         | 4.30  |        | 38.49                       | 14.50      | 53.00            |              |         | 1.29  |        | 38.45                       | 11.73      | 50.18            |              |
|         | 4.09  |        | 40.03                       | 29.05      | 69.07            |              |         | 1.24  |        | 39.11                       | 17.09      | 56.20            |              |
|         | 3.95  |        | 41.25                       | 214.93     | 256.19           |              |         | 1.20  |        | 39.79                       | 40.65      | 80.44            |              |
|         | 3.78  |        | 42.08                       | 485.51     | 527.59(62.7)     |              |         | 1.17  |        | 40.39                       | 85.97      | 126.36(91.6)     |              |
|         | 3.78  |        | 50.16                       | 1362.40    | 1412.6           |              |         | 1.17  |        | 51.43                       | 1450.22    | 1501.6           |              |

**Table 2:** Leakage/delay tradeoffs from dual  $T_{ox}$  optimization. For each circuit, Row 1 = all transistors @ $T_{oxHi}$ , Row 5 = all transistors @ $T_{oxLo}$ , Rows 2–4 = results for intermediate target delays. Row 4 matches the delay for the “all  $T_{oxLo}$ ” point with a leakage savings of “%R,” and “%D” in Row 1 shows the delay penalty of the all  $T_{oxHi}$  case relative to this point. Each row shows  $I_{gate}$ ,  $I_{sub}$  and  $I_{total}$ , and the CPU time required to generate the entire leakage-delay tradeoff curve is in the last column.

Table 2 shows leakage/delay tradeoffs for all ISCAS85 benchmarks (except the smallest, C17), including values of  $I_{sub}$ ,  $I_{gate}$ , and  $I_{total}$  for various target delays. The all- $T_{oxHi}$  case typically has a delay penalty of about 25% as compared  $I_{sub}$  and  $I_{gate}$  typically increase, the latter being at a much more rapid rate. The delay corresponding to all transistors @ $T_{oxLo}$  can be matched, with an average reduction, over all circuits, of 82.7% in  $I_{total}$ , with the minimum reduction being 62.7% for C6288. In each case, the knee point on the curve fares far better. The other data points show that our optimization technique yields a tradeoff curve that results in a smooth tradeoff as the total leakage increases from the all- $T_{oxHi}$  case, with a delay reduction that is in the range of about 20%.

## 7. CONCLUSION

We have presented a technique for reducing the total active leakage, including gate oxide leakage, by determining appropriate values of  $T_{ox}$ , and iteratively assigning them to the individual transistor in the circuit. Our approach shows a clear tradeoff between leakage and delay, and an achievable delay reduction of 20%.

## 8. REFERENCES

- [1] Semiconductor Industry Association, “International Technology Roadmap for Semiconductors,” 2002. Available at <http://public.itrs.net>.
- [2] F. Hamzaoglu and M. R. Stan, “Circuit-Level Techniques to Control Gate Leakage for Sub-100 nm CMOS,” in *Proc. of ACM/IEEE ISLPED*, pp. 60–63, Aug. 2002.
- [3] D. Lee and D. Blaauw, “Static Leakage Reduction through Simultaneous Threshold Voltage and State Assignment,” in *Proc. of ACM/IEEE DAC*, pp. 191–194, Jun. 2003.
- [4] J. Kao *et al.*, “Transistor Sizing Issues and Tool for Multi-Threshold CMOS Technology,” in *Proc. of ACM/IEEE DAC*, pp. 409–414, Jun. 1997.
- [5] Y. Oowaki *et al.*, “A sub-0.1  $\mu m$  Circuit Design with Substrate-Over-Biasing,” in *IEEE ISSCC Dig. of Tech. Papers*, pp. 88–89, Feb. 1998.
- [6] S. Narendra *et al.*, “Leakage Issues in IC design: Trends, Estimation, and Avoidance.” Tutorial at the IEEE/ACM ICCAD, Nov. 2003.
- [7] D. Lee *et al.*, “Analysis and Minimization Techniques for Total Leakage Considering Gate Oxide Leakage,” in *Proc. of ACM/IEEE DAC*, pp. 175–180, Jun. 2003.
- [8] C.-H. Choi *et al.*, “Impact of Gate Direct Tunneling on Circuit Performance: A Simulation Study,” *IEEE Trans. on Electron Devices*, pp. 2823–2829, Dec. 2001.
- [9] N. Sirisantana *et al.*, “High-Performance Low-Power CMOS Circuits Using Multiple Channel Length and Multiple Oxide Thickness,” in *Proc. of IEEE ICCD*, pp. 227–232, Sept. 2000.
- [10] K. Bernstein, Private Communication. IBM T. J. Watson Research Center, Yorktown Heights, NY, 2003.
- [11] Y. Taur, “CMOS Design Near the Limits of Scaling,” *IBM J. R&D*, vol. 46(2/3), pp. 213–222, Mar./May 2002.
- [12] K. Chen *et al.*, “Predicting CMOS Speed with Gate Oxide and Voltage Scaling and Interconnect Loading Effects,” *IEEE Trans. On Electron Devices*, vol. 44(11), pp. 1951–1957, Nov. 1997.
- [13] Device Group at UC Berkeley, “Berkeley Predictive Technology Model,” 2002. Available at <http://www-device.eecs.berkeley.edu/~ptm/>.
- [14] S. Sirichotiyakul *et al.*, “Duet: An Accurate Leakage Estimation and Optimization Tool for Dual- $V_t$  Circuits,” *IEEE Trans. on VLSI Systems*, vol. 10(2), pp. 79–90, Apr. 2002.
- [15] A. Chandrakasan *et al.*, *Design of High-Performance Microprocessor Circuits*. Piscataway, NJ: IEEE Press, 2001.
- [16] K. A. Bowman *et al.*, “A Circuit-Level Perspective of the Optimum Gate Oxide Thickness,” *IEEE Trans. on Electron Devices*, vol. 48(8), pp. 1800–1810, Aug. 2001.
- [17] J. Fishburn and A. Dunlop, “TILOS: A Polynomial Programming Approach to Transistor Sizing,” in *Proc. of ACM/IEEE ICCAD*, pp. 326–328, Nov. 1985.
- [18] E. M. Sentovich *et al.*, “SIS: A System for Sequential Circuit Synthesis,” Tech. Rep. UCB/ERL M92/41, Electronics Research Laboratory, Dept. of EECS, University of California, Berkeley, May 1992.